

Published in final edited form as:

*Aging Cell*. 2014 February ; 13(1): 92–101. doi:10.1111/ace.12150.

## Maintenance of Muscle Mass and Load-Induced Growth in Muscle RING Finger 1 Null Mice with Age

Darren T. Hwee<sup>1,3</sup>, Leslie M. Baehr<sup>2</sup>, Andrew Philp<sup>1</sup>, Keith Baar<sup>1,2</sup>, and Sue C. Bodine<sup>1,2</sup>

<sup>1</sup>Department of Neurobiology, Physiology, and Behavior, Cellular and Integrative Physiology Graduate Group University of California, Davis, Davis, CA, 95616

<sup>2</sup>Department of Physiology and Membrane Biology, Cellular and Integrative Physiology Graduate Group University of California, Davis, Davis, CA, 95616

<sup>3</sup>Molecular, Cellular and Integrative Physiology Graduate Group University of California, Davis, Davis, CA, 95616

### Summary

Age-related loss of muscle mass occurs to varying degrees in all individuals and has a detrimental effect on morbidity and mortality. Muscle Ring Finger 1 (MuRF1), a muscle specific E3 ubiquitin ligase, is believed to mediate muscle atrophy through the ubiquitin proteasome system (UPS). Deletion of MuRF1 (KO) in mice attenuates the loss of muscle mass following denervation, disuse and glucocorticoid treatment; however, its role in age-related muscle loss is unknown. In this study, skeletal muscle from male wild type (WT) and MuRF1 KO mice were studied up to the age of 24 months. Muscle mass and fiber cross-sectional area decreased significantly with age in WT, but not KO mice. In aged WT muscle, significant decreases in proteasome activities, especially 20S and 26S  $\beta 5$  (20–40% decrease), were measured and were associated with significant increases in the maladaptive endoplasmic reticulum (ER) stress marker, CHOP. Conversely, in aged MuRF1 KO mice 20S or 26S  $\beta 5$  proteasome activity was maintained or decreased to a lesser extent than in WT mice and no increase in CHOP expression was measured. Examination of the growth response of older (18 months) mice following functional overload, revealed that WT mice had significantly less growth relative to young mice (1.37 vs. 1.83 fold), whereas MuRF1 KO mice had a normal growth response (1.74 vs. 1.90 fold). These data collectively suggest that with age, MuRF1 plays an important role in the control of skeletal muscle mass and growth capacity through the regulation of cellular stress.

### Keywords

Sarcopenia; Ubiquitin Proteasome System; Anabolic Resistance; ER Stress

### Introduction

Muscle Ring Finger 1, MuRF1, is a muscle specific E3 ubiquitin ligase that is transcriptionally increased in skeletal muscle in response to a variety of stressors that induce muscle atrophy (Bodine et al., 2001). Deletion of MuRF1 in skeletal muscle has been shown to attenuate the loss of muscle mass under catabolic conditions including: denervation, disuse, and glucocorticoid treatment (Baehr et al., 2011; Gomes et al., 2012; Labeit et al., 2010). MuRF1 functions as an E3 ubiquitin ligase, and thus it has been predicted that muscle

sparing in mice with a null deletion of MuRF1 (i.e., MuRF1 KO) would be related to a decrease in proteasome activity. However, a recent study revealed that muscle sparing following denervation is associated with significant increases, not decreases, in both 20S and 26S proteasome subunit activities in MuRF1 KO versus wild type (WT) mice (Gomes et al., 2012). Furthermore, deletion of MuRF1 was shown to influence Akt/mTOR mediated signaling and protein synthesis (Baehr et al., 2011; Hwee et al., 2011). Given the muscle sparing effects of MuRF1 deletion and the possibility that MuRF1 has a role in the regulation of protein quality control, we examined whether mice with a null deletion of MuRF1 demonstrated sparing of muscle mass and load-induced growth as a consequence of aging.

Sarcopenia is the age-related loss of muscle mass and function that occurs to a varying extent in all individuals and can lead to frailty and a decrease in mobility and quality of life (Janssen et al., 2002). A major factor believed to contribute to age-related muscle loss is a change in protein turnover. The ubiquitin proteasome system (UPS) is a tightly regulated system responsible for intracellular protein turnover, including the removal of short-lived normal proteins as well as misfolded and dysfunctional proteins (Koga et al., 2011). The maintenance of proteasome activity and subsequent protein turnover is believed to be necessary for proper cellular function (Wong and Cuervo, 2010). For example, altered proteasome function and the subsequent accumulation of ubiquitin-tagged proteins and protein aggregates have been implicated in the pathology of several neurodegenerative diseases including Parkinson's disease, Alzheimer's disease and Huntington's disease (Riederer et al., 2011; Vernace et al., 2007). Like other cell types, skeletal muscle fibers maintain a continual state of protein renewal through dynamic rates of protein synthesis and degradation. The aging process has been associated with a decrease in proteasome activity in several tissues including brain, liver, and cardiac muscle however, in skeletal muscle controversy exists regarding whether proteasome activity is increased, decreased or unchanged as a function of age (Koga et al., 2011; Low, 2011; Patterson et al., 2007). A number of studies have reported a decrease in proteasome activity in skeletal muscles with advanced age (Ferrington et al., 2005; Husom et al., 2004; Lee et al., 1999; Strucksberg et al., 2010); however, others have reported an age-associated increase in proteasome activity (Altun et al., 2010; Hepple et al., 2008). In the present study, we measured the  $\beta$ 1,  $\beta$ 2 and  $\beta$ 5 20S and 26S proteasome subunit activities in aged (24 month), but not senescent WT and MuRF1 KO mice. Given our recent data showing that proteasome activity is enhanced in the MuRF1 KO mice following denervation (Gomes et al., 2012), we hypothesized that with aging, deletion of MuRF1 would result in an elevated level of proteasome activity that would be associated with muscle sparing.

The present study revealed a significant difference in the response of WT and MuRF1 KO mice to aging. Specifically, we found that the growth response to loading was impaired in aged WT mice, but maintained in MuRF1 KO mice. Further, we found that muscle mass and fiber cross-sectional area were maintained in the MuRF1 KO mice with advanced age. A major finding was that both 20S and 26S proteasome activities decreased significantly with age in WT mice. In contrast, the activities of the majority of the proteasome subunits in the old MuRF1 KO mice were significantly higher than the activities measured in the old WT mice. Overall, the data suggest that deletion of MuRF1 maintains protein quality control in skeletal muscle, leading to reductions in endoplasmic reticulum and oxidative stress and the maintenance of muscle mass and growth capacity.

## Results

### MuRF1 deletion spares muscle mass and fiber cross-sectional area and increases capillary density with age

Given that muscle mass is spared in MuRF1 KO mice following denervation and other atrophy-inducing conditions, we examined whether MuRF1 KO mice were resistant to age-related muscle loss. Skeletal muscle mass, fiber cross-sectional area and maximum isometric force were similar in WT and MuRF1 KO mice up to the age of 18 months (Fig. 1, Table 1). At 24 months of age, significant muscle atrophy occurred in WT mice as measured by a decrease in muscle mass, fiber area and maximum isometric tension (Fig. 1, Table 1). In contrast, 24m KO mice had no decrease in muscle mass or fiber cross-sectional area relative to young adult KO mice. Unexpectedly, maximum isometric tension was significantly down in the 24m KO mice even though there was significant sparing of muscle mass. Moreover, the age-associated decrease in tension output was greater in the KO than the WT mice (Suppl Fig. 1). Given that tension was measured via direct nerve stimulation, the drop in tension output may reflect denervation or a decrease in synaptic efficacy. Analysis of the isometric twitch revealed a slowing of both time-to-peak tension and half relaxation time in both WT and KO mice (Suppl Table 1). Another characteristic of aging muscle that was examined in WT and KO mice was capillary density. Capillary density was not significantly different in WT and KO mice at 18m or younger; however, at 24m capillary density significantly increased in the MuRF1 KO mice resulting in a significant difference between KO and WT mice (Fig. 2A, Suppl Fig. 2). Interestingly, expression of HIF-1 $\alpha$  protein was significantly higher in KO than WT mice at both 18 and 24 months. Moreover, there was a significant increase in HIF-1 $\alpha$  expression in KO mice between 18 and 24 months (Fig. 2B).

### MAFbx expression is elevated in MuRF1 KO, but not WT mice with aging

The expression of select genes associated with denervation and aging was assessed in young (6m) and old (24m) WT and KO mice (Fig. 2C). No significant changes were observed for FOXO1 or MuRF1 expression with age. Embryonic myosin heavy chain, a gene associated with inactivity and regeneration, was elevated significantly in both old WT and KO mice. MAFbx, a muscle-specific E3 ligase associated with denervation and atrophy, significantly increased with age in the KO, but not WT mice. Expression of CHIP, an ubiquitin ligase that promotes the degradation of unfolded proteins, was slightly elevated in old KO ( $p=0.06$ ), but not WT ( $p=0.11$ ) mice.

### The ubiquitin proteasome system is maintained in aged MuRF1 KO mice

Accumulation of ubiquitinated and damaged proteins occurs in muscle with aging and has been associated with a decrease in the UPS (Combaret et al., 2009). Here, we found that polyubiquitinated proteins increased significantly in both WT and KO muscle as a function of age, as assessed by western blot and ELISA (Fig. 3). Next, we measured the ATP-dependent (26S) and ATP-independent (20S) activities of the catalytic subunits ( $\beta$ 1,  $\beta$ 2,  $\beta$ 5) in the gastrocnemius muscle of young (6m) and old (24m) WT and KO mice (Fig. 3C). In WT mice, the activities of all 20S and 26S catalytic subunits, except for the 26S  $\beta$ 2, significantly decreased with age, accounting for the observed accumulation of polyubiquitinated proteins. For the majority of subunits (4 of 6), proteolytic activity was significantly higher in the old KO than WT mice.

To determine whether the change in proteasome subunit activity was related to alterations in the amount of proteasome, western blots were performed for specific 19S (RPT6, RPT1) and 20S ( $\beta$ 5, PSMA6) proteasome subunits. No age-related changes were observed for any of the subunits in WT or KO mice (Suppl Fig 3). Measurement of the inducible subunits  $\beta$ 1i and  $\beta$ 5i did reveal age-related changes in both WT and KO mice. A significant increase in

$\beta$ 1i expression was measured in both WT and KO mice with age, while  $\beta$ 5i expression significantly increased only in WT mice with age. (Suppl Fig. 3). Expression of PA28 $\alpha$  was greater in KO than WT adult mice (9m), however, PA28 $\alpha$  expression was similar in old (24m) WT and KO mice due to a significant increase in expression in the WT mice from 9 to 24 months of age (Suppl Fig 3).

### **Oxidative and ER Stress are differentially regulated in WT and MuRF1 KO mice with age**

To determine whether there was an increase in oxidative stress with age, the level of oxidatively modified proteins was measured in the gastrocnemius of young and old WT and KO mice (Fig. 4A). In young mice, the amount of oxidized proteins was significantly lower in MuRF1 KO than WT mice. With age, however, the level of oxidized proteins significantly increased in the KO, but not WT mice. Increases in oxidative stress have been associated with increases in calpain and caspase-3 activities, which were subsequently measured in young and old mice (Fig. 4B, C) (Nelson et al., 2012; Whidden et al., 2010). Calpain (I and II) activity was similar in WT and KO mice at 6m, and significantly decreased in both WT and KO mice at 24m. In contrast, caspase-3 activity was similar in WT and KO mice at 6m, but significantly increased at 24m in the KO mice only. Interestingly, levels of the anti-apoptosis protein, Bcl-2, were significantly higher in the KO mice at 24m (Fig 4D).

Endoplasmic reticulum (ER) stress, as measured by BiP, PDI and CHOP expression was also examined as a function of age in the WT and KO mice (Fig. 5). Both of the adaptive stress markers, BiP and PDI, increased significantly as a function of age (6m vs. 24m) in WT and KO mice. In contrast, the maladaptive marker, CHOP, increased significantly at 24m in WT, but not KO, mice.

### **The growth response to functional overload is blunted in aging WT, but not MuRF1 KO mice**

Aging not only results in a loss of muscle mass, but also anabolic resistance, i.e., the inability to respond to growth cues. The growth response of skeletal muscle to increased mechanical loading is attenuated in aging rodents as early as 18 month of age (Hwee and Bodine, 2009). Thus, we examined the growth response of the plantaris muscle from young (6m) and older (18–20m) WT and MuRF1 KO mice to increase mechanical loading using the functional overload (FO) model. At 18 month of age, WT and KO mice had similar muscle mass and demonstrated no age-related muscle loss (Table 1). Following 14 days of overload, growth of the plantaris was similar in young WT and KO mice (Fig 6A). In contrast, older WT mice showed a significant decrease in the amount of growth relative to young mice (1.37 vs 1.83 fold), while older KO mice had a growth response that was similar to the young mice (1.74 vs. 1.90 fold). To further examine the dynamics of the growth response, we measured the response of older WT and KO mice to 7 and 14 days of overload. These experiments revealed that during the first 7 days of overload muscle growth was similar in old WT and KO mice, however, between 7 and 14 days muscle growth plateaued in the WT mice, while muscle growth continued in the KO mice (Fig. 6B). Previous publications have shown that with age activation of the Akt/mTOR signaling pathway is blunted leading to attenuated muscle hypertrophy in response to mechanical load (Hwee and Bodine, 2009; Thomson and Gordon, 2006). In this study, we found that after 7 days of overload activation of both PKB/Akt and S6K1 was significantly higher in KO compared to WT mice (Fig 6C, Suppl. Fig. 4).

In skeletal muscle, ER stress mediates anabolic resistance through PKB/Akt inhibition (Deldicque et al., 2011). The accumulation of unfolded or misfolded proteins in the ER can occur during periods of high rates of synthesis, as occur during functional overload (Zhang

and Kaufman, 2006). Examination of the expression of the adaptive and maladaptive ER stress markers revealed a significant increase in ER stress in response to overload in both WT and KO mice (Fig. 6D, E). Of particular interest was the finding that the maladaptive ER stress response, as denoted by CHOP levels, increased to a greater extent in both young and old WT compared to KO mice following overload.

## Discussion

Muscle Ring Finger-1 (MuRF1), a muscle specific E3 ubiquitin ligase, is an atrophy-associated gene that is transcriptionally increased following denervation and disuse, two processes associated with aging (Bodine et al., 2001). The extent to which MuRF1 is involved in the aging process is controversial since both no change (Gaugler et al., 2011; Leger et al., 2008) and increased (Clavel et al., 2006) expression of MuRF1 has been reported in aging muscle. A key finding in this study was that the activities of both the 20S and 26S proteasomal subunits decreased significantly with age in WT mice, but were maintained or decreased to a lesser extent in the MuRF1 KO mice with age. Further, we demonstrate that the absence of MuRF1 results in the maintenance of two properties shown to decrease with age, i.e. muscle mass and skeletal muscle growth in response to increased loading, which suggests that MuRF1 expression plays an important role in the regulation of skeletal muscle mass and function with age. These data are contrary to prevailing theory that age-related loss of muscle mass is caused by an increase in the ubiquitin proteasome system (Altun et al., 2010). Instead, these data suggest that a decrease in proteasome activity with aging contributes to cellular dysfunction in skeletal muscle, as indicated by an increase in ER stress. The current findings support the theory that maintaining or increasing protein turnover decreases cellular dysfunction and is beneficial to maintaining muscle mass during aging.

**The ubiquitin proteasome system and age-related muscle loss**—The UPS is responsible for the removal of short-lived, dysfunctional, and misfolded proteins (Koga et al., 2011). Its role in protein turnover is critical for optimal cell performance, as a decrease in proteasome activity has been shown to lead to an accumulation of protein aggregates and overall cellular dysfunction (Wong and Cuervo, 2010). Increases in UPS activity are implicated in a number of conditions that induce skeletal muscle atrophy and are believed to play a role in age-related muscle loss (Combaret et al., 2009). Aging is a slow progressive process that leads to decreases in skeletal muscle mass and strength; contributing to increases in morbidity and mortality. Although it is generally accepted in other tissues that the UPS decreases with aging, its activity in skeletal muscle with aging is less clear, as both increases (Altun et al., 2010; Hepple et al., 2008) and decreases (Ferrington et al., 2005; Husom et al., 2004; Strucksberg et al., 2010) in proteasome activity have been reported in aging muscle. The present study measured the 20S and 26S proteasome activities of all three ( $\beta$ 1,  $\beta$ 2,  $\beta$ 5) subunits in old mice (24 months) on a C57Bl6 background and found a significant decrease in the activity in 5 of 6 of the subunits. In MuRF1 KO mice, the activity of 4 of these subunits and overall  $\beta$ 5 activity was higher in the KO mice than the WT. The higher proteasome activities in the aged MuRF1 KO versus WT mice could be playing a role in the observed maintenance of muscle mass and fiber cross-sectional area with age. Recently, we reported that muscle sparing in the MuRF1 KO mice following denervation was associated with an increase, not a decrease in proteasome activity relative to WT mice (Gomes et al., 2012). The idea that elevated proteasome activity is beneficial for cellular function is not new, and several recent studies have shown that impairment of proteasome activity is harmful to muscle (Anvar et al., 2011). Recently, a transgenic mouse was developed with decreased proteasome chymotrypsin-like ( $\beta$ 5) activity and showed a shortened life span and a decrease in muscle mass (Haas et al., 2007; Tomaru et al., 2012). Mice with a deletion of carboxyl terminus of HSP70-interacting protein (CHIP) also

demonstrate a shortened life span and accelerated loss of skeletal muscle mass, and coincidentally have defects in protein quality control and an accelerated loss of chymotrypsin-like ( $\beta 5$ ) activity with age (Min et al., 2008). Interestingly, we observed an increase in the expression of CHIP, as well as MAFbx, in the aged KO mice.

The mechanism responsible for the elevated proteasome activity in the old MuRF1 KO is unknown. One factor that could be contributing to the lack of inactivation of proteasome activity in the MuRF1 KO mice with age is the increased MAFbx expression. In a previous study we noted that in response to neural inactivity, the absence of MuRF1 results in sustained elevated levels of MAFbx expression, suggesting that MuRF1 is involved in a feedback loop that controls MAFbx expression (Gomes et al., 2012). Of relevance to the current study, was the finding that following denervation, proteasome activity was higher in the MuRF1 KO compared to WT mice. It is possible that the elevated proteasome activity in the old MuRF1 KO mice is linked to neural inactivity. The mechanism by which MuRF1 deletion spares muscle mass under conditions of inactivity may be related to an increased ability to decrease cellular stress and maintain global protein synthesis.

**The reciprocal UPS and ER Stress Relationship**—One potential consequence of diminished proteasome capacity is the accumulation of misfolded or dysfunctional proteins that compromise endoplasmic reticulum associated protein degradation (ERAD). The accumulation of misfolded or unfolded proteins in the endoplasmic reticulum can lead to ER stress and the unfolded protein response (Fu et al., 2008). The initial ER stress response is adaptive yielding an increase in the protein folding capacity of the cell and a decrease in protein translation. When the unfolded protein response fails, however, cells may initiate a maladaptive response, i.e., apoptosis. We found that aged WT muscle had increased BiP, a chaperone protein indicative of the adaptive ER stress response, and CHOP, a pro-apoptotic marker of the maladaptive ER stress response. In contrast, in old MuRF1 KO muscle BiP levels were high in the absence of changes in CHOP levels. Interestingly, we found an increase in caspase-3 activity in the old KO mice. Classically, caspase-3 has been used as an indicator of increases in apoptosis. However, in muscle, the elevated caspase-3 could be involved in an increase in myofilament turnover (Du et al., 2004) and proteasome activation (Wang et al., 2010), which is consistent with the elevated proteasome activity seen in the MuRF1 KO mice. Our observed increase in the anti-apoptosis marker Bcl-2 in the MuRF1 KO mice with age could suggest a mechanism to protect the muscle from the apoptotic affects of increased caspase-3.

Overall, the data suggest that deletion of MuRF1 results in reduced levels of cellular stress. In young mice the amount of oxidized proteins was significantly lower in MuRF1 KO mice than WT mice. With age, ER stress increased in the WT mice without an apparent increase in the amount of oxidized proteins. In contrast, the amount of oxidized proteins significantly increased in the MuRF1 KO mice with age, without an increase in the maladaptive ER stress response but an increase in the adaptive ER stress response. The elevated oxidative stress in the MuRF1 KO mice could be the result of denervation (discussed below), however, it appears that the MuRF1 KO mice are capable of increasing anti-oxidant defenses that protect the muscle from atrophy. Increases in HIF-1 $\alpha$ , caspase-3, and Bcl-2 expression and proteasome activity in the old MuRF1 KO mice could all be playing a role in reducing ER stress and protecting the muscle from atrophy.

**MuRF1 Expression and Age-Associated Loss of Muscle Mass**—The loss of MuRF1 expression results in muscle sparing under a number of atrophy inducing condition, including denervation (Baehr et al., 2011; Gomes et al., 2012). The present results reveal that the deletion of MuRF1 also has a positive impact on the aging process resulting in the sparing of muscle mass and the retention of the growth response. Aging is associated with

anabolic resistance, i.e., the loss of the ability to increase muscle mass in response to anabolic signals such as increased loading, which is attributed to a decrease in the activation of mTORC1-mediated signaling and protein translation. The retention of the load-induced growth response in the MuRF1 KO mice was associated with less ER stress and greater activation of PKB/Akt and S6K1, a downstream target of mTORC1, relative to WT mice and suggests that there was greater activation of protein translation in the old MuRF1 KO compared to WT mice. The attenuation of load-induced growth occurs with aging (Hwee and Bodine, 2009) and diet-induced obesity (Sitnick et al., 2009), and is related to a decrease or delay in the activation of Akt and mTORC1-signaling. In mice, S6K1 activation peaks at around 7 days following functional overload in young mice, however, in the present study we observed a reduced and delayed activation of S6K1 in the old WT mice and normal activation of S6K1 in the old MuRF1 KO mice. The pattern of Akt and S6K1 activation observed in the old WT mice following FO is consistent with previously observations in old rats and DIO mice, which have a reduced load-induced growth response (Hwee and Bodine, 2009; Sitnick et al., 2009). Our data suggest that deletion of MuRF1 leads to less cellular stress and the ability to maintain a net positive protein balance in aged animals in response to increased loading. Previous data have demonstrated that elevated ER Stress can inhibit the Akt/mTORC1 signaling and protein translation in skeletal muscle (Deldicque et al., 2011). Additional experiments are required to directly test the hypothesis that the ability to induce a normal growth response in muscle from old MuRF1 KO mice is related to a reduced level of ER stress, leading to greater activation of protein translation.

**MuRF1 and the Neuromuscular Junction**—One perplexing finding is the fact that muscle force output, as measured *in situ* through stimulation of the nerve, was significantly less in the old MuRF1 KO mice relative to the old WT mice. At 18 months of age, the maximum isometric force output of the WT and KO mice is similar, however, by 24 months force output is diminished in both the WT and KO mice with a greater decrease in the KO than WT mice. These data might suggest a greater loss of myofilament proteins in the KO relative to the WT mice, however, the fiber CSA was higher in the MuRF1 animals and the relative amount of myosin heavy chain and actin were similar in the old MuRF1 and WT KO mice (data not shown). Another explanation could be that there is more denervation or synaptic instability in the old MuRF1 KO mice compared to the WT mice. Synaptic remodeling occurs as early as 18 months of age in C57BL6 mice as neuromuscular junctions begin to lose innervation and either become reinnervated or remain denervated (Valdez et al., 2010). We have observed that following denervation in the MuRF1 KO mice, there is a decrease in expression of myogenin and acetylcholine receptor subunits (manuscript in submission). The suppression of various activity-associated genes could stabilize the neuromuscular junction and inhibit reinnervation in the MuRF1 KO mice during this time of motoneuron loss and synapse remodeling. Interestingly, a recent paper reports that MuRF1 controls the turnover of the acetylcholine receptor (AChR) (Rudolf et al., 2012). Under normal fully innervated conditions, no difference was found in the turnover of the AChR in WT and MuRF1 KO mice, however, following denervation, turnover of the AChR was significantly higher in the WT compared to the KO mice. Our observations in aging MuRF1 KO mice suggest that a lack of synaptic remodeling may suppress reinnervation resulting in chronically denervated muscle fibers, however, this theory requires further investigation.

In conclusion, the deletion of the MuRF1 gene and protein expression is beneficial to muscle during aging. The mechanism of action appears to be through the maintenance of protein quality control and suppression of cellular stress. These data highlight the need for additional efforts to identify the *in vivo* substrates of MuRF1 in skeletal muscle and to determine the mechanism by which MuRF1 functions to reduce cellular stress and maintain muscle mass and growth capacity

## Experimental Procedures

### Animals

The generation of mice with a null deletion of MuRF1 has been previously described (Bodine et al., 2001). Homozygous knockout (KO) and wild type (WT) mice were obtained by intercrossing heterozygous MuRF1 mice. A total of 78 male mice, ranging in age from 6 to 24 months were used in this study. Mice were kept under a 12h light-dark cycle and were fed standard diets. The Institutional Animal Care and Use Committee at the University of California, Davis approved all animal protocols used in this study.

### Functional Overload Model

The plantaris muscle in both legs was overloaded by the surgical removal of its major synergists: the soleus and medial and lateral gastrocnemius muscles. Animals were anesthetized with isoflurane gas and prepared for surgery using aseptic procedures. Mice were given buprenorphine post surgery for pain and monitored on a daily basis until the muscles were removed 7–14 days post surgery.

### Histology

The gastrocnemius complex (soleus, medial and lateral gastrocnemius, plantaris) was excised, cleaned, pinned to corkboard, and frozen in melting isopentane. Serial cross-sections (10  $\mu$ m) were stained with hematoxylin and eosin for evaluation of general histology, anti-laminin (Sigma 1:1000) for the measurement of fiber cross-sectional area, and CD31 for the measurement of capillary density. Digital images were taken under 200 $\times$  total magnification and analyzed by Axiovision software (Zeiss). For each muscle, six nonoverlapping regions of the triceps surae complex were analyzed (~600 fibers/ muscle sections).

### RNA isolation and quantitative PCR

Total RNA was isolated from mechanically homogenized muscle in 1ml of Trizol reagent. All centrifuge steps were performed at 12,000 rpm at 4°C. Homogenized samples were centrifuged for 15 minutes, and the resulting top aqueous layer was transferred to a microcentrifuge tube containing 200  $\mu$ l of chloroform. After a 15 min incubation period, the samples were centrifuged for 15 minutes. The top aqueous layer was added to 0.5 ml of isopropyl alcohol, mixed well, and centrifuged for 10 min. The RNA pellet was washed with 75% ethanol, air-dried, and resuspended in DEPC water for RT-PCR analysis. cDNA was made using a Quantitect Reverse Transcription Kit (Qiagen, Valencia, CA). The resulting cDNA was analyzed by quantitative PCR with unlabeled primers in SYBR Green PCR Master Mix (Applied Biosystems, Foster City, CA) for 40 cycles at an annealing temperature of 59°C. Each sample was run in triplicate. The following primer sequences were used in this study: MuRF1: 5'-GCTGGTGGAAAACATCATTGACAT-3' and 5'-CATCGGGTGGCTGCCTTT-3'; MAFbx: 5'-GACTGGACTTCTCGACTGCC-3' and 5'-TCAGGGATGTGAGCTGTGAC-3'; FOXO1: 5'-AAGAGCGTGCCCTACTTCAA-3' and 5'-TGCTGTGAAGGGACAGATTG-3'; eMHC: 5'-ACT TCA CCT CTA GCC GGA TG-3' and 5'-ATT GTC AGG AGC CAC GAA A-3'; Rpl39: 5'-CAAAATCGCCCTATTCCTCA-3' and 5'-AGACCCAGCTTCGTTCTCCT-3'.

### Western Blots

Muscle tissue was homogenized in sucrose lysis buffer. 10–20  $\mu$ g were prepared in Laemmli sample loading buffer, separated by SDS-page, and transferred to a polyvinylidene difluoride membrane. Equal loading was verified by ponceau stain. The membranes were incubated overnight at 4°C in 1X Tris-buffered saline-Tween (TBST) with the appropriate



antibodies: Following three rinses in 1× TBST, membranes were incubated with corresponding secondary antibodies (Vector and Pierce). After three additional washes, membranes were visualized with chemiluminescent substrate (Millipore). Protein Oxidation was measured using the OxiSelect™ Protein Carbonyl Immunoblot Kit according to the manufacturer's instructions, except a 1:2000 dilution was made for the Anti-DNP antibody instead of the recommended 1:1000 (Cell Biolabs). A total of 10 µg of protein was loaded onto a 10% SDS-PAGE gel. Immobilon Western Chemiluminescent HRP substrate (Millipore) was used to detect the oxidized proteins. Image acquisition and band quantification was performed using the ChemiDoc™ MP System and Image Lab 4.1 software (Biorad). The following antibodies were used in this study: Actin (0.5 ng/mL, Sigma), anti-polyubiquitin (1:2000, FK1, Biomol), PA28α (1:1000, Biomol), β1i (1:1000, Biomol), RPT6 and β5i (1:1000, commercially made and affinity purified by 21<sup>st</sup> Century Biochemicals), β5 (1:1250, Biomol), PSMA6 (1:1000, Epitomics), RPT1 (1:1000, Enzo Life Sciences), HIF-1α (1:500, Santa Cruz), total S6K1 (1:1000, Santa Cruz), and BiP (1:1000, BD Biosciences). CHOP (1:1000), PDI (1:1000), phospho S6K1 (1:1000), phospho and total AKT (1:1000), Bcl2 (1:1000) and B-actin (1:5000) were obtained from Cell Signaling.

### ELISA-based measurements of polyubiquitinated proteins

Muscle homogenate (1 µg) was incubated overnight at 4°C to optimize binding to the bottom of 96-well ELISA plates (Santa Cruz Biotech). Samples were incubated in blocking buffer (1% BSA/1× PBST), rinsed three times in 1× PBS and incubated with anti-polyubiquitin (1:2000, FK1, Biomol). Following three rinses in 1× PBST, secondary antibody conjugated to horseradish peroxidase (HRP) was added. TMB substrate was added to initiate a color change reaction proportional to HRP activity, and 2.5M sulfuric acid was added to stop the reaction. The quantification of polyubiquitinated proteins was measured spectrophotometrically at a wavelength of 450 nm. Absorbance values for wells containing 1% BSA were used as background controls. The specificity of the polyubiquitin antibody was validated with purified ubiquitin and a penta-ubiquitinated chain (Biomol) (Hwee et al., 2011).

### Proteasome Activity

20S and 26S proteasome activity assays were performed as previously described (Gomes et al., 2006). All assays were carried out in a total volume of 100µl in 96-well opaque plates. The final composition of the 20S assay buffer was 250 mM HEPES, 5mM EDTA, and 0.03% SDS (pH 7.5). The final composition of the 26S assay buffer was 50 mM Tris, 1 mM EDTA, 150 mM NaCl, 5 mM MgCl<sub>2</sub>, 50 µM ATP, and 0.5 mM dithiothreitol (pH 7.5). Powdered muscle was homogenized by a dounce tissue grinder in 26S buffer. Samples were centrifuged for 30 minutes at 12,000g. The resulting supernatant was used to assess proteasome activity. The individual caspase-like (β1), trypsin-like (β2), and chymotrypsin-like (β5) activity of the 20S and 26S proteasome were measured by calculating the difference between fluorescence units recorded with or without the specific inhibitors in the reaction medium. β1 was initiated by the addition of 10 µl of 1mM Z-Leu-Leu-Glu-7-AMC (Peptides Int.); β2 by 10 µl of 1 mM Boc-Leu-Ser-Thr-Arg-7-amido-4-methylcoumarin (Bachem); and β5 by 10 µl of 1mM of succinyl-Leu-Leu-Val-Tyr-7-amido-4-methylcoumarin (LLVY-AMC) (Bachem). The β1, β2, and β5 subunit assays were conducted in the absence and presence of their respective inhibitors: 40 nM Z-Pro-Nle-Asp-al (Biomol), 40 µM Epoxomicin, and 10 µM epoxomicin (Peptides Int.). These substrates were cleaved by the proteasome subunits releasing free AMC. Released AMC was measured using a Fluoroskan Ascent fluorometer (Thermo Electron) at an excitation wavelength of 390 nm and an emission wavelength of 460 nm. Fluorescence was measured at 15-minute intervals for 2 hours. All assays were linear in this range and each sample was assayed in quadruplicate.

### Caspase-3 Activity

Caspase-3 activity was measured fluorometrically in 96-well opaque plates. 50 µg of protein supernatant was added to an assay buffer containing 100 mM HEPES, 0.2% CHAPS, 200mM NaCl, 2mM EDTA, 20% glycerol (v/v), fresh 20 mM dithiothreitol (pH 7.4). Caspase activation was initiated by the addition of 100 µM of caspase-3 substrate Ac-DEVD-AMC (Biomol). This substrate is cleaved by caspase-3, releasing free AMC which is detected fluorometrically by a Fluoroskan Ascent fluorometer (Thermo Electron) at an excitation wavelength of 390 nm and an emission wavelength of 460 nm. Caspase-3 activity was measured by calculating the difference between fluorescence units recorded with or without caspase inhibitor 10 µM Ac-DEVD-CHO (Biomol). Fluorescence was measured at 15-minute intervals for 2 hours. All assays were linear in this range and each sample was assayed in quadruplicate. Activity is expressed as mean ± S.E.M.

### Calpain Activity

Calpain activity was measured fluorometrically in 96-well opaque plates. 50 µg of protein supernatant was added to an assay buffer containing 50 mM Tris, 1 mM EDTA, 10 mM CaCl<sub>2</sub>, 150 mM NaCl, and fresh 0.5 mM dithiothreitol (pH 7.4). Calpain activity was initiated by the addition of 200 µM of substrate LLVY-AMC (Bachem). This substrate is cleaved by calpain, releasing free AMC which is detected fluorometrically by a Fluoroskan Ascent fluorometer (Thermo Electron) at an excitation wavelength of 390 nm and an emission wavelength of 460 nm. Calpain activity was measured by calculating the difference between fluorescence units recorded in the presence and absence of 50 µM calpain inhibitor IV (Calbiochem). Fluorescence was measured at 15-minute intervals for 2 hours. All assays were linear in this range and each sample was assayed in quadruplicate. Activity is expressed as mean ± S.E.M. This assay measures both calpain I and II activity.

### Statistical analysis

Two-way ANOVA was performed to access the effect of age and genotype using Sigma Stat 3.1 (Systat Software, San Jose, CA). Tukey's post hoc analysis was used to determine differences when interactions existed. A one-way ANOVA was performed to determine significance in cases where only one independent variable (age or genotype) was being examined. Results are expressed as mean ± S.E.M., with significance set as  $p < 0.05$ .

### Supplementary Material

Refer to Web version on PubMed Central for supplementary material.

### Acknowledgments

This research was supported by grants from the Muscular Dystrophy Association and the National Institutes of Health (DK75801). Partial support for DTH was provided by HHMI-IMBS56006769 and T32HL086350 training fellowships.

### References

- Altun M, Besche HC, Overkleeft HS, Piccirillo R, Edelmann MJ, Kessler BM, Goldberg AL, Ulfhake B. Muscle wasting in aged, sarcopenic rats is associated with enhanced activity of the ubiquitin proteasome pathway. *The Journal of biological chemistry*. 2010; 285:39597–39608. [PubMed: 20940294]
- Anvar SY, t Hoen PA, Venema A, van der Sluijs B, van Engelen B, Snoeck M, Vissing J, Trollet C, Dickson G, Chartier A, et al. Deregulation of the ubiquitin-proteasome system is the predominant molecular pathology in OPMD animal models and patients. *Skeletal muscle*. 2011; 1:15. [PubMed: 21798095]

- Baehr LM, Furlow JD, Bodine SC. Muscle Sparing in Muscle RING Finger 1 Null Mice: Response to Synthetic Glucocorticoids. *The Journal of physiology*. 2011; 589:4759–4776. [PubMed: 21807613]
- Bodine SC, Latres E, Baumhueter S, Lai VK, Nunez L, Clarke BA, Poueymirou WT, Panaro FJ, Na E, Dharmarajan K, et al. Identification of ubiquitin ligases required for skeletal muscle atrophy. *Science*. 2001; 294:1704–1708. [PubMed: 11679633]
- Clavel S, Coldefy AS, Kurkdjian E, Salles J, Margaritis I, Derijard B. Atrophy-related ubiquitin ligases, atrogin-1 and MuRF1 are up-regulated in aged rat Tibialis Anterior muscle. *Mechanisms of ageing and development*. 2006; 127:794–801. [PubMed: 16949134]
- Combaret L, Dardevet D, Bechet D, Taillandier D, Mosoni L, Attaix D. Skeletal muscle proteolysis in aging. *Curr Opin Clin Nutr Metab Care*. 2009; 12:37–41. [PubMed: 19057185]
- Deldicque L, Bertrand L, Patton A, Francaux M, Baar K. ER stress induces anabolic resistance in muscle cells through PKB-induced blockade of mTORC1. *PLoS one*. 2011; 6:e20993. [PubMed: 21698202]
- Du J, Wang X, Miereles C, Bailey JL, Debigare R, Zheng B, Price SR, Mitch WE. Activation of caspase-3 is an initial step triggering accelerated muscle proteolysis in catabolic conditions. *The Journal of clinical investigation*. 2004; 113:115–123. [PubMed: 14702115]
- Ferrington DA, Husom AD, Thompson LV. Altered proteasome structure, function, and oxidation in aged muscle. *FASEB journal: official publication of the Federation of American Societies for Experimental Biology*. 2005; 19:644–646. [PubMed: 15677694]
- Fu HY, Minamino T, Tsukamoto O, Sawada T, Asai M, Kato H, Asano Y, Fujita M, Takashima S, Hori M, et al. Overexpression of endoplasmic reticulum-resident chaperone attenuates cardiomyocyte death induced by proteasome inhibition. *Cardiovasc Res*. 2008; 79:600–610. [PubMed: 18508854]
- Gaugler M, Brown A, Merrell E, Disanto-Rose M, Rathmacher JA, Reynolds TH. PKB Signaling and AtroGene Expression in Skeletal Muscle of Aged Mice. *J Appl Physiol*. 2011; 111:192–199. [PubMed: 21551011]
- Gomes AV, Waddell DS, Siu R, Stein M, Dewey S, Furlow JD, Bodine SC. Upregulation of proteasome activity in muscle RING finger 1-null mice following denervation. *FASEB journal: official publication of the Federation of American Societies for Experimental Biology*. 2012; 26:2986–2999. [PubMed: 22508689]
- Gomes AV, Zong C, Edmondson RD, Li X, Stefani E, Zhang J, Jones RC, Thyparambil S, Wang GW, Qiao X, et al. Mapping the murine cardiac 26S proteasome complexes. *Circ Res*. 2006; 99:362–371. [PubMed: 16857966]
- Haas KF, Woodruff E 3rd, Broadie K. Proteasome function is required to maintain muscle cellular architecture. *Biology of the cell/under the auspices of the European Cell Biology Organization*. 2007; 99:615–626. [PubMed: 17523916]
- Hepple RT, Qin M, Nakamoto H, Goto S. Caloric restriction optimizes the proteasome pathway with aging in rat plantaris muscle: implications for sarcopenia. *American journal of physiology Regulatory, integrative and comparative physiology*. 2008; 295:R1231–1237.
- Husom AD, Peters EA, Kolling EA, Fugere NA, Thompson LV, Ferrington DA. Altered proteasome function and subunit composition in aged muscle. *Archives of biochemistry and biophysics*. 2004; 421:67–76. [PubMed: 14678786]
- Hwee DT, Bodine SC. Age-related deficit in load-induced skeletal muscle growth. *The journals of gerontology Series A, Biological sciences and medical sciences*. 2009; 64:618–628.
- Hwee DT, Gomes AV, Bodine SC. Cardiac Proteasome Activity in Muscle Ring Finger-1 Null Mice at Rest and Following Synthetic Glucocorticoid Treatment. *Am J Physiol Endocrinol Metab*. 2011; 301:E967–E977. [PubMed: 21828340]
- Janssen I, Heymsfield SB, Ross R. Low relative skeletal muscle mass (sarcopenia) in older persons is associated with functional impairment and physical disability. *J Am Geriatr Soc*. 2002; 50:889–896. [PubMed: 12028177]
- Koga H, Kaushik S, Cuervo AM. Protein homeostasis and aging: The importance of exquisite quality control. *Ageing research reviews*. 2011; 10:205–215. [PubMed: 20152936]

- Labeit S, Kohl CH, Witt CC, Labeit D, Jung J, Granzier H. Modulation of muscle atrophy, fatigue and MLC phosphorylation by MuRF1 as indicated by hindlimb suspension studies on MuRF1-KO mice. *Journal of biomedicine & biotechnology*. 2010; 2010:693741. [PubMed: 20625437]
- Lee CK, Klopp RG, Weindruch R, Prolla TA. Gene expression profile of aging and its retardation by caloric restriction. *Science*. 1999; 285:1390–1393. [PubMed: 10464095]
- Leger B, Derave W, De Bock K, Hespel P, Russell AP. Human sarcopenia reveals an increase in SOCS-3 and myostatin and a reduced efficiency of Akt phosphorylation. *Rejuvenation research*. 2008; 11:163–175B. [PubMed: 18240972]
- Low P. The role of ubiquitin-proteasome system in ageing. *Gen Comp Endocrinol*. 2011; 172:39–43. [PubMed: 21324320]
- Min JN, Whaley RA, Sharpless NE, Lockyer P, Portbury AL, Patterson C. CHIP deficiency decreases longevity, with accelerated aging phenotypes accompanied by altered protein quality control. *Molecular and cellular biology*. 2008; 28:4018–4025. [PubMed: 18411298]
- Nelson WB, Smuder AJ, Hudson MB, Talbert EE, Powers SK. Cross-talk between the calpain and caspase-3 proteolytic systems in the diaphragm during prolonged mechanical ventilation. *Critical care medicine*. 2012; 40:1857–1863. [PubMed: 22487998]
- Patterson C, Ike C, Willis PWt, Stouffer GA, Willis MS. The bitter end: the ubiquitin-proteasome system and cardiac dysfunction. *Circulation*. 2007; 115:1456–1463. [PubMed: 17372187]
- Riederer BM, Leuba G, Vernay A, Riederer IM. The role of the ubiquitin proteasome system in Alzheimer's disease. *Exp Biol Med (Maywood)*. 2011; 236:268–276. [PubMed: 21383047]
- Rudolf R, Bogomolovas J, Strack S, Choi KR, Khan MM, Wagner A, Brohm K, Hanashima A, Gasch A, Labeit D, et al. Regulation of nicotinic acetylcholine receptor turnover by MuRF1 connects muscle activity to endo/lysosomal and atrophy pathways. *Age (Dordr)*. 2012
- Sitnick M, Bodine SC, Rutledge JC. Chronic high fat feeding attenuates load-induced hypertrophy in mice. *The Journal of physiology*. 2009; 587:5753–5765. [PubMed: 19822547]
- Strucksberg KH, Tangavelou K, Schroder R, Clemen CS. Proteasomal activity in skeletal muscle: a matter of assay design, muscle type, and age. *Analytical biochemistry*. 2010; 399:225–229. [PubMed: 20034461]
- Thomson DM, Gordon SE. Impaired overload-induced muscle growth is associated with diminished translational signalling in aged rat fast-twitch skeletal muscle. *The Journal of physiology*. 2006; 574:291–305. [PubMed: 16627569]
- Tomaru U, Takahashi S, Ishizu A, Miyatake Y, Gohda A, Suzuki S, Ono A, Ohara J, Baba T, Murata S, et al. Decreased proteasomal activity causes age-related phenotypes and promotes the development of metabolic abnormalities. *The American journal of pathology*. 2012; 180:963–972. [PubMed: 22210478]
- Valdez G, Tapia JC, Kang H, Clemenson GD Jr, Gage FH, Lichtman JW, Sanes JR. Attenuation of age-related changes in mouse neuromuscular synapses by caloric restriction and exercise. *Proceedings of the National Academy of Sciences of the United States of America*. 2010; 107:14863–14868. [PubMed: 20679195]
- Vernace VA, Schmidt-Glenewinkel T, Figueiredo-Pereira ME. Aging and regulated protein degradation: who has the UPPER hand? *Aging cell*. 2007; 6:599–606. [PubMed: 17681036]
- Wang XH, Zhang L, Mitch WE, LeDoux JM, Hu J, Du J. Caspase-3 cleaves specific 19 S proteasome subunits in skeletal muscle stimulating proteasome activity. *The Journal of biological chemistry*. 2010; 285:21249–21257. [PubMed: 20424172]
- Whidden MA, Smuder AJ, Wu M, Hudson MB, Nelson WB, Powers SK. Oxidative stress is required for mechanical ventilation-induced protease activation in the diaphragm. *J Appl Physiol*. 2010; 108:1376–1382. [PubMed: 20203072]
- Wong E, Cuervo AM. Integration of clearance mechanisms: the proteasome and autophagy. *Cold Spring Harb Perspect Biol*. 2010; 2:a006734. [PubMed: 21068151]
- Zhang K, Kaufman RJ. Protein folding in the endoplasmic reticulum and the unfolded protein response. *Handb Exp Pharmacol*. 2006:69–91. [PubMed: 16610355]

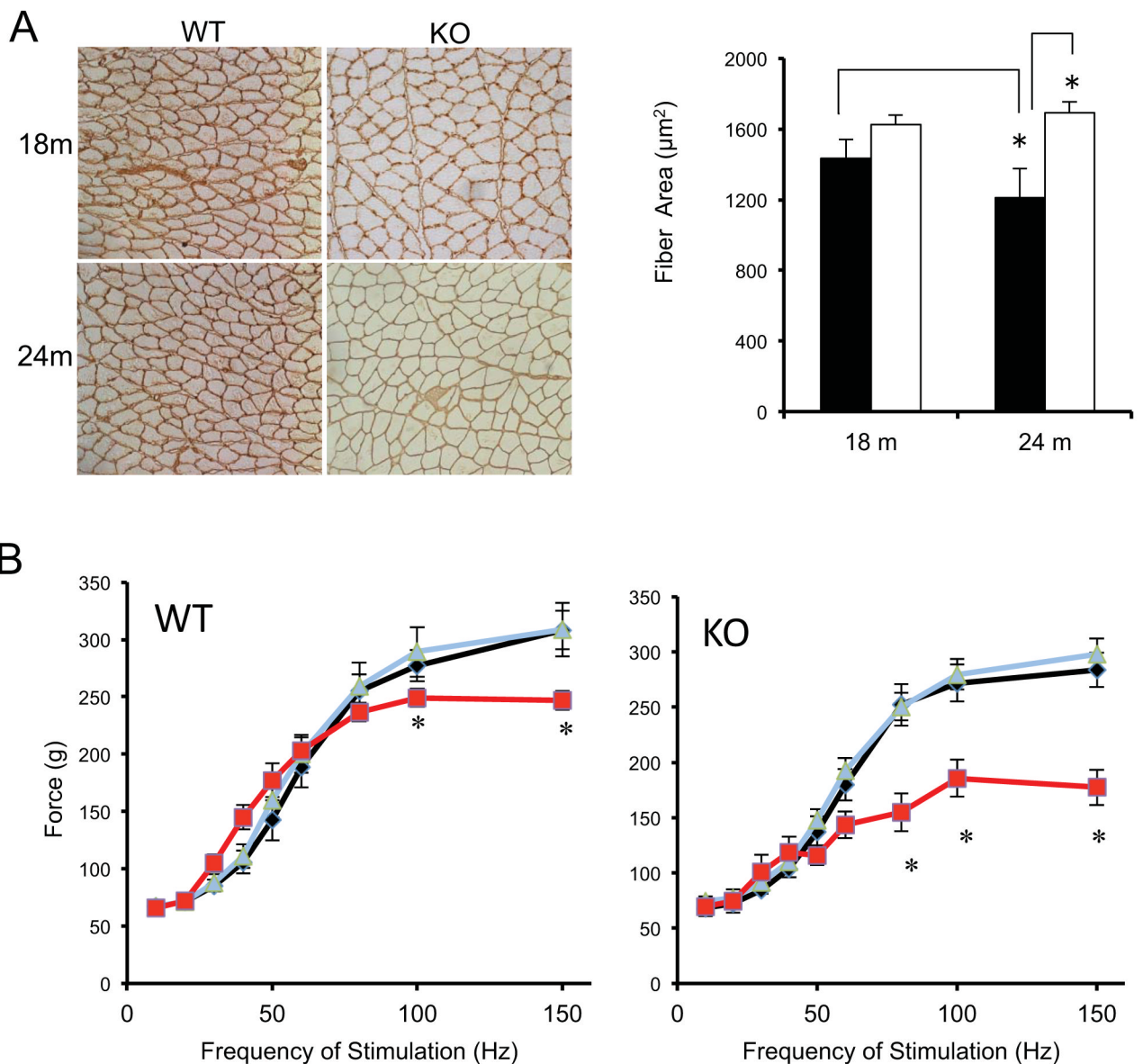


**Figure 1. Maintenance of muscle mass in MuRF1 KO mice with aging**

(A) Representative laminin-stained sections from 18 and 24 month old WT and MuRF1 KO mice. (B) Average fiber cross-sectional area of the gastrocnemius muscle (medial and lateral heads) of WT (black) and MuRF1 KO (white) at 18 and 24 months. (C) In situ isometric contractile force measurements of the gastrocnemius muscle of WT and MuRF1 KO mice at 8 (black), 18 (blue) and 24 (red) months of age. Data are mean  $\pm$  SEM, n = 5 mice per group. Statistical significance was set at  $p < 0.05$  and determined using a two-way ANOVA for CSA and one-way ANOVA for force output.

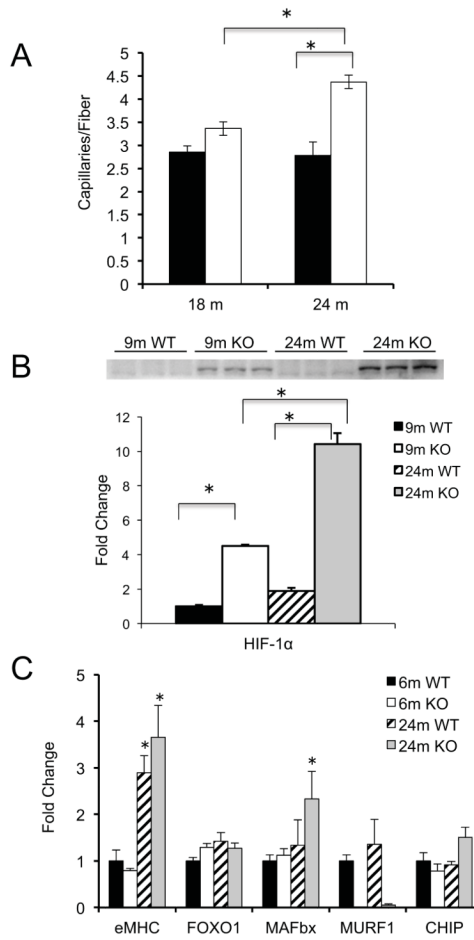


**Figure 2. Capillary Density and Differential Gene Expression in WT and MuRF1 KO mice with age**  
 (A) Capillary density, measured as the number of capillaries per muscle fiber, was determined in the medial and lateral gastrocnemius muscle from CD31 stained cross-sections in 18 and 24 month old WT (black) and KO (white) mice. (B) Representative western blot of HIF-1 $\alpha$  from homogenates of the gastrocnemius complex taken from young adult (9m) and old (24m) WT and MuRF1 KO mice. Means  $\pm$  SEM (n=4 per group) are expressed as a fold change relative to the 9m WT mean. (C) The mRNA expression levels of selected genes were determined from homogenates of the gastrocnemius complex of young (6m) and old (24m) WT and MuRF1 KO mice. Means ( $\pm$ SEM, n 4 per group) are expressed as a fold change relative to the 6m WT mean. Statistical significance was set at  $p < 0.05$  and determined using a two-way ANOVA.

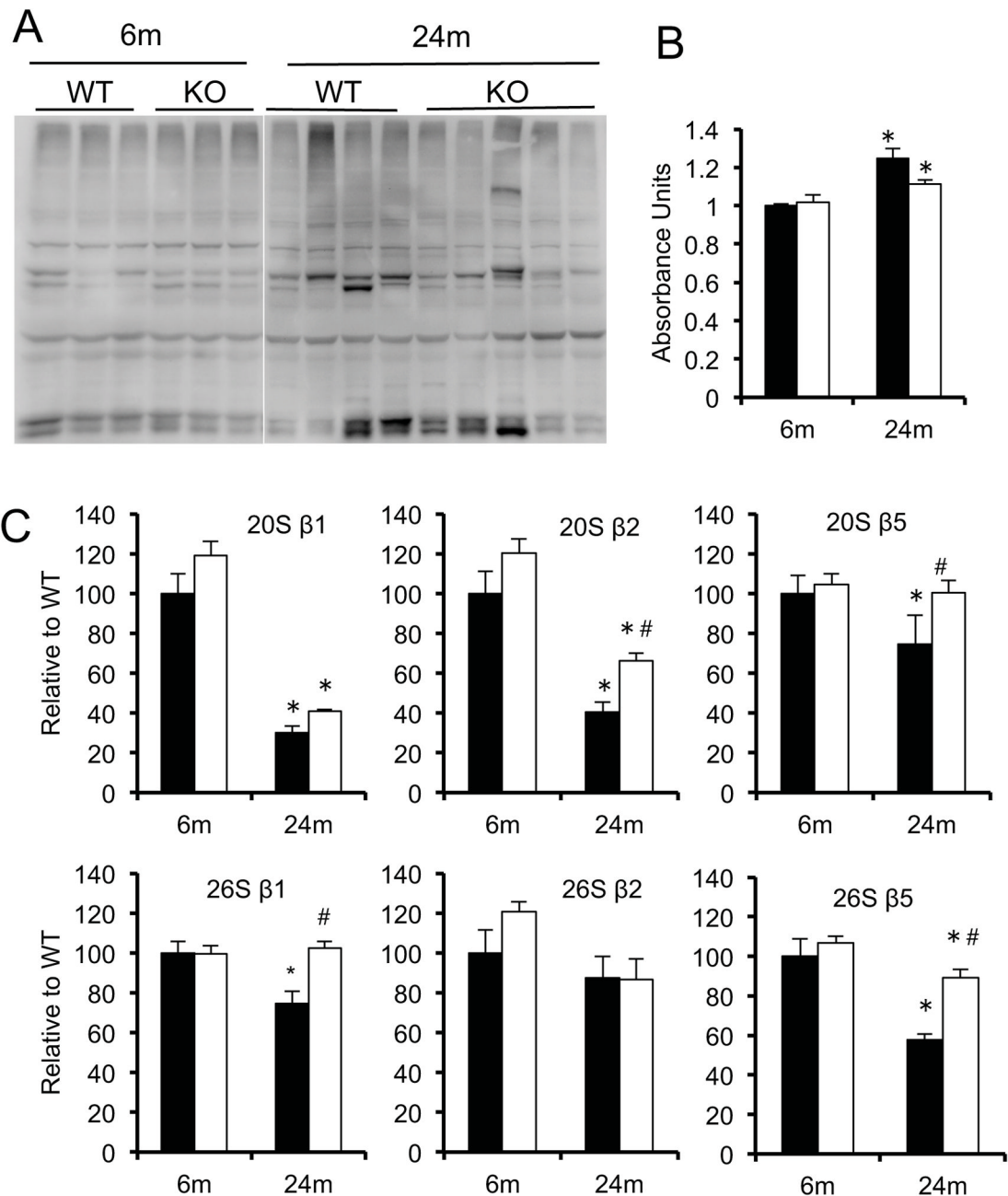


**Figure 3. Higher levels of proteasome activity in MuRF1 KO mice relative to WT with aging**  
 (A) Western blots of lysates from the gastrocnemius complex of young (6m, n=3) and old (24m, n=4) WT and MuRF1 KO mice. Polyubiquitinated proteins were determined by immunoblotting with an anti-ubiquitin antibody (FK1). (B) Polyubiquitin levels were quantified by ELISA in 6m and 24 m old wild type (black) and MuRF1 KO (white). Data are mean  $\pm$  SEM for n=4–5 per group. (C) ATP-dependent (26S) and ATP-independent (20S) proteasome activities in lysates from the gastrocnemius complex of WT (black) and MuRF1 KO (white) mice at 6 and 24 months. Individual subunit activities are shown for:  $\beta$ 1, caspase-like activity;  $\beta$ 2, trypsin-like activity; and  $\beta$ 5, chymotrypsin-like activity. Data are mean  $\pm$  SEM, n=4 mice per group. Statistical significance was set at  $p < 0.05$  and determined using a two-way ANOVA. \* indicates significant difference between young and old within a

specific genotype, # indicates significant difference between WT and KO mice at a given age.



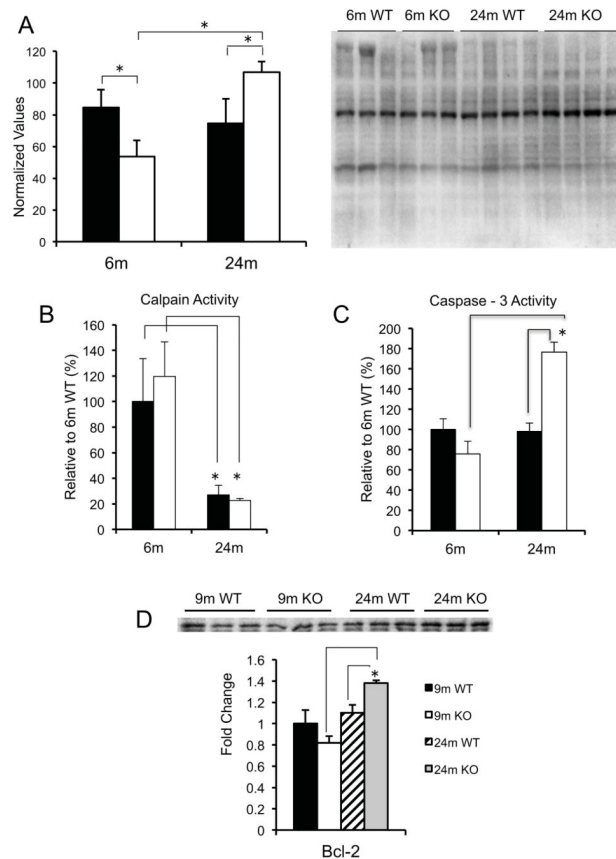


#### Figure 4. Oxidative stress in WT and KO mice

(A) Oxidized proteins were measured in the gastrocnemius muscle of young (6m) and old (24m) WT (black) and KO (white) mice using the OxiSelect™ Protein Carbonyl Immunoblot Kit. Data are mean  $\pm$  SEM,  $n=3-4$  mice. Calpain (B) and Caspase-3 (C) activity were measured in the gastrocnemius of WT (black) and KO (white) mice. Means  $\pm$  SEM are expressed as a percent of 6m WT mean. (D) Western blot of Bcl-2 from homogenates of the gastrocnemius taken from young adult (9m) and old (24m) WT and MuRF1 KO mice. Means  $\pm$  SEM ( $n=3$  per group) are expressed as a fold change relative to the 6m WT mean. Statistical significance was set at  $p<0.05$  and determined using a two-way ANOVA.

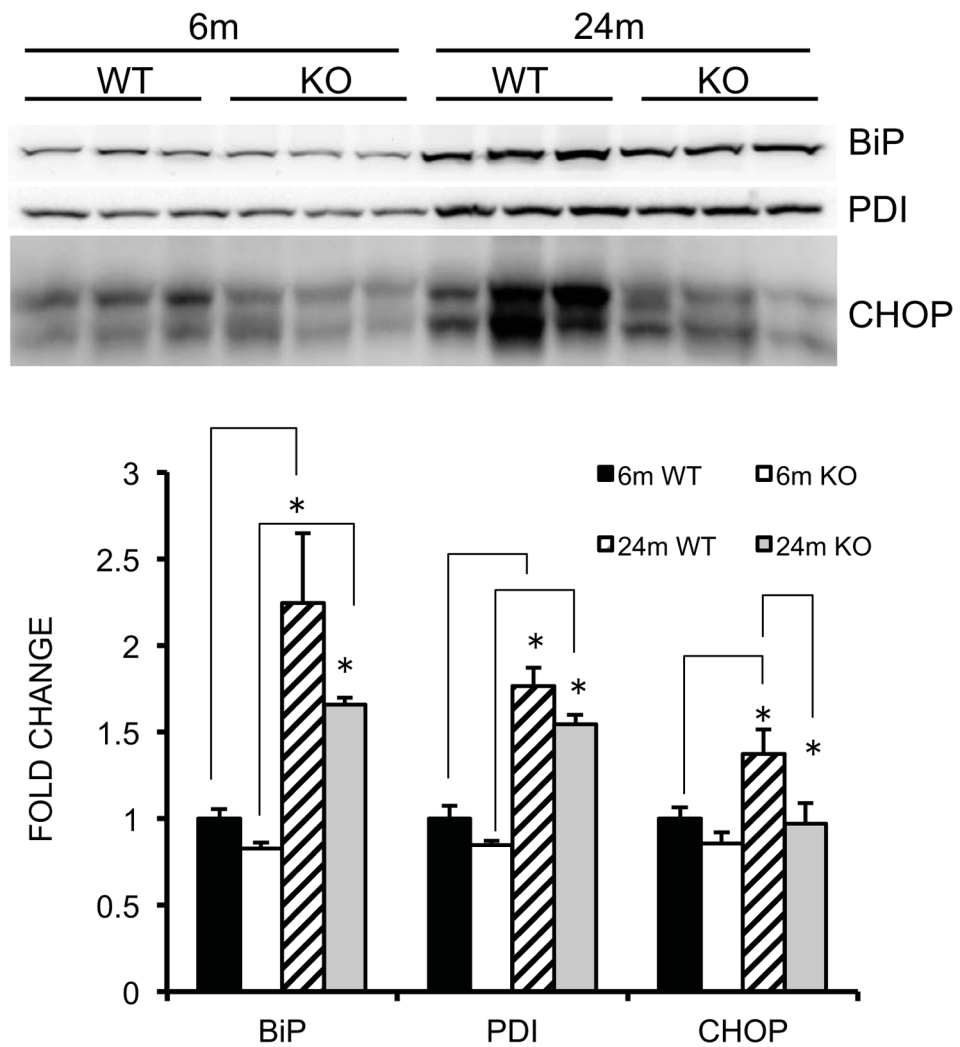


**Figure 5. Markers of endoplasmic reticulum (ER) stress are elevated in old WT, but not MuRF1 KO mice**

Representative western blots of ER stress markers (BiP, PDI, and CHOP) from homogenates of the gastrocnemius taken from young adult (6m) and old (24m) WT and MuRF1 KO mice. Means  $\pm$  SEM (n=4 per group) are expressed as a fold change relative to the 6m WT mean. Statistical significance was set at  $p < 0.05$  and determined using a two-way ANOVA.

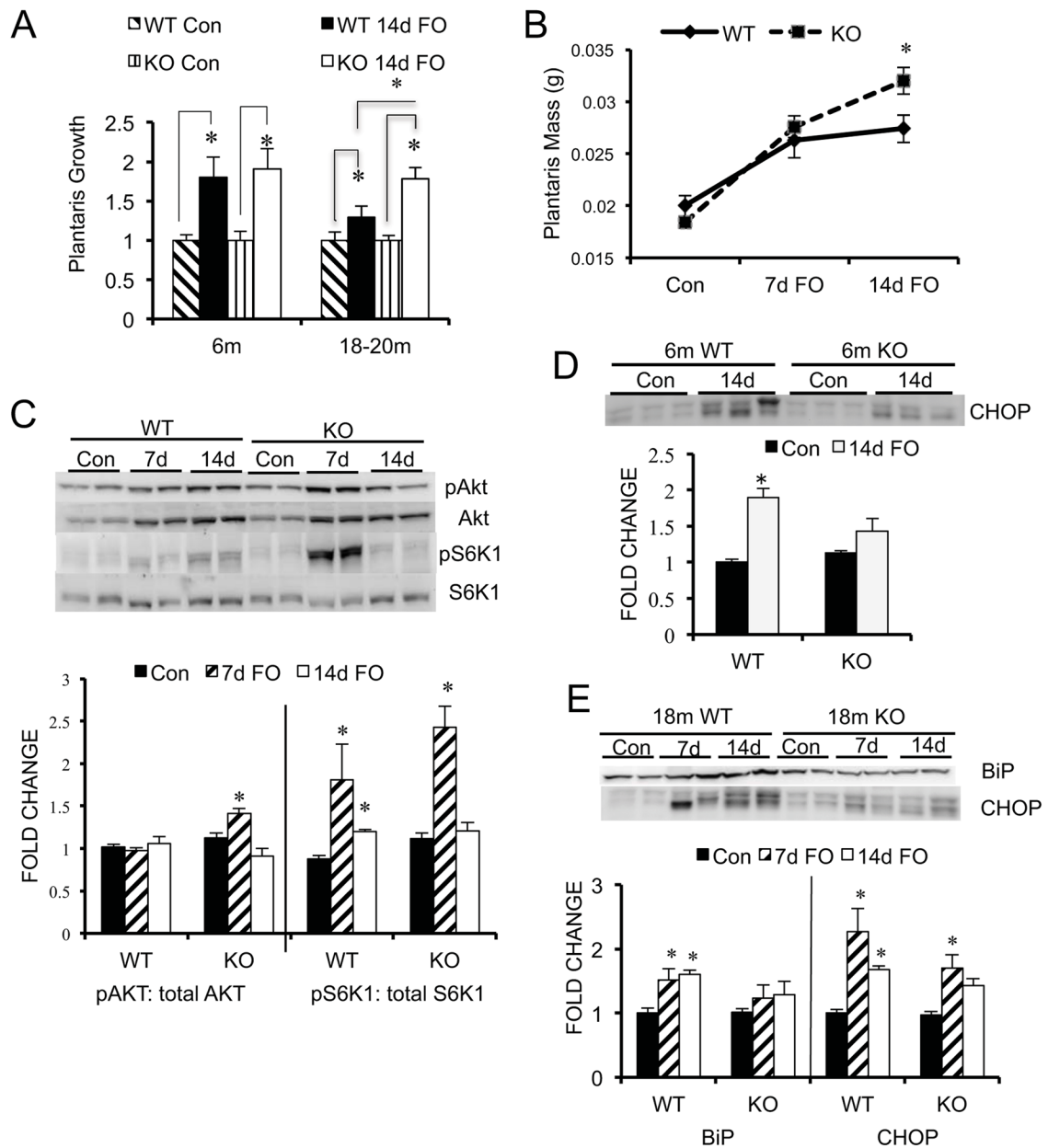


**Figure 6. Load-induced growth is maintained in older MuRF1 KO mice compared to WT mice** (A) Growth of the plantaris muscle (fold change relative to control, mean  $\pm$  SEM,  $n=5$ ) following 14 days of functional overload (FO) in young (6m) and older (18–20m) WT (black) and MuRF1 KO (white) mice. (B) Growth of the plantaris muscle (wet weight in grams) following 7 and 14 days of FO in 18–20 month old WT (solid) and MuRF1 KO (dashed) mice. (C) Representative western blots ( $n=2$ ) and quantification ( $n=4$ ) of the phosphorylation levels of Akt and S6K1 in the plantaris muscle of old (18–20 m) WT and KO mice following no treatment (Con, black) and FO for 7 (hatched) and 14 (white) days. (D) Representative western blot ( $n=3$ ) and quantification ( $n=5$ ) of CHOP protein levels in the plantaris of young WT and MuRF1 KO mice following no treatment (Con, black) and 14 days of FO (white). (E) Representative western blot ( $n=2$ ) and quantification ( $n=4$ ) of BiP and CHOP protein levels in the plantaris of older (18 m) WT and MuRF1 KO mice

following no treatment (Con, black) and FO for 7 (hatched) and 14 days (white). Data are expressed as a fold change relative to WT control (mean  $\pm$  SEM). Statistical significance was set at  $p < 0.05$  and determined using a two-way ANOVA for growth and a one-way ANOVA for protein expression.

**Table 1**

Body Weight and Muscle Mass of WT and MuRF1 KO animals

	<b>BW (g)</b>	<b>Heart (g)</b>	<b>TA (g)</b>	<b>GA complex (g)</b>
6m WT	31.9 ± 1.8	0.144 ± .006	0.054 ± .002	0.183 ± .007
6m KO	35.7 ± 2.1	0.175 ± .005*	0.056 ± .002	0.193 ± .004
12m WT	35.4 ± 1.4	0.158 ± .004 <sup>a</sup>	0.058 ± .001	0.192 ± .003
12m KO	32.0 ± 1.1	0.210 ± .003*,#	0.056 ± .001	0.199 ± .003
18m WT	36.7 ± 3.7	0.168 ± .007		0.173 ± .003
18m KO	36.2 ± 2.0	0.208 ± .004		0.181 ± .005
24m WT	36.4 ± 0.8	0.179 ± .005 <sup>#</sup>	0.051 ± .002	0.159 ± .006 <sup>#</sup>
24m KO	39.1 ± 1.3	0.247 ± .008*,#	0.055 ± .001	0.184 ± .004*

Body weight (BW), heart and hindlimb skeletal muscle (tibialis anterior (TA), gastrocnemius (GA) complex (medial and lateral gastrocnemius, soleus, and plantaris) masses (wet weight) from WT and MuRF1 KO male mice at 6, 12, 18 and 24 months of age. Values are expressed as mean ± SEM. A two-way ANOVA was performed with Tukey's post hoc analysis. Statistical significance was set at  $p < 0.05$ ;

\* indicates significant difference between WT and KO mice at a specific age;

# indicates significance difference between ages within a specific genotype.